HHS Public Access

Author manuscript

Cell Stem Cell. Author manuscript; available in PMC 2016 June 04.

Published in final edited form as:

Cell Stem Cell. 2015 June 4; 16(6): 627–638. doi:10.1016/j.stem.2015.04.013.

Krt19(+)/*Lgr5*(−) cells are radioresistant cancer initiating stem cells in the colon and intestine

Samuel Asfaha[1,7], **Yoku Hayakawa**[1], **Ashlesha Muley**[1], **Sarah Stokes**[1], **Trevor A. Graham**[3], **Russell Ericksen**[1], **Christoph B. Westphalen**[1], **Johannes von Burstin**[5], **Teresa L. Mastracci**[4], **Daniel L. Worthley**[1], **Chandhan Guha**[6], **Michael Quante**[5], **Anil K. Rustgi**[2], and **Timothy C. Wang**[1]

[1]Division of Digestive and Liver Diseases, Department of Medicine, Irving Cancer Research Center, Columbia University, New-York; New York, USA; 10032

[2]Division of Gastroenterology, Department of Medicine, Abramson Cancer Center, University of Pennsylvania; Philadelphia, PA 19104

[3]Centre for Tumour Biology, Barts Cancer Institute; London; UK; EC1M 6BQ

[4]Department of Genetics and Development, Columbia University, New York; NY; USA; 10032

[5]II. Medizinische Klinik, Klinikum rechts der Isar, Technische Universität München; Munich; Germany; 81675

[1]Correspondence to: Timothy C. Wang, MD; 1130 St. Nicholas Avenue, Room 925, New York, NY 10032, Phone: (212) 851-4581; Fax: (212) 851-4590; tcw21@columbia.edu.

The authors do not have any conflicts of interests to declare.

Author Contributions:

Samuel Asfaha:	study concept and design, acquisition of data, analysis and interpretation of data; writing of manuscript
Yoku Hayakawa:	acquisition of data, analysis
Ashlesha Muley	acquisition of data, analysis
Sarah Stokes:	acquisition of data, analysis
Trevor Graham:	analysis and interpretation of data
Russell Ericksen:	acquisition of data, analysis
Christoph B. Westphalen:	acquisition of data, analysis
Johannes von Burstin:	acquisition of data, analysis
Teresa L. Mastracci:	acquisition of data, analysis
Daniel L. Worthley:	analysis and writing of manuscript
Chandan Guha	analysis and interpretation of data
Michael Quante:	analysis and interpretation of data
Anil K. Rustgi:	analysis and writing of manuscript
Timothy C. Wang:	study concept, analysis and interpretation of data; writing of manuscript

[6]Department of Radiation Oncology, Albert Einstein College of Medicine; New York; NY; USA; 10467

[7]Department of Medicine, University of Western Ontario; London; Ontario; Canada; N6A 5W9

Abstract

The colonic and intestinal epithelium are renewed every 3 days. In the intestine there are at least two principal stem cell pools. The first contains rapid cycling crypt based columnar (CBC) *Lgr5*$^+$ cells, while the second is comprised of slower cycling *Bmi1*-expressing cells at the +4 position above the crypt base. In the colon, however, the identification of *Lgr5*-negative stem cell pools has proven more challenging. Here, we demonstrate that the intermediate filament, *keratin*-19 (*Krt19*), marks long-lived, radiation resistant cells above the crypt base that generate *Lgr5*$^+$ CBCs in the colon and intestine. In colorectal cancer models, *Krt19*$^+$ cancer initiating cells are also radioresistant while *Lgr5*$^+$ stem cells are radiosensitive. Moreover, *Lgr5*$^+$ stem cells are dispensable in both the normal and neoplastic colonic epithelium, as ablation of *Lgr5*$^+$ stem cells results in their regeneration from *Krt19* expressing cells. Thus, *Krt19*$^+$ stem cells are a discrete target relevant for cancer therapy.

Graphical Abstract

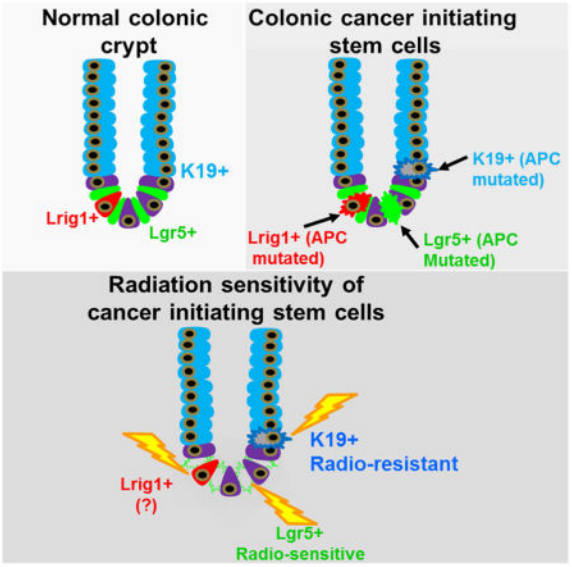

Keywords

Krt19; intestine; colon; stem cells; cancer

Introduction

Adult tissue stem cells are characterized by multipotentiality and the capacity to self-renew (Li and Clevers, 2010). In the mouse small intestine and colon, the simple columnar epithelium is rapidly renewed every 3 days. Genetic inducible fate mapping studies suggest

that epithelial cells in the small intestine are replaced from at least two principal stem cell pools, comprising both rapidly cycling crypt based columnar (CBC) *Lgr5*-expressing cells, and slower cycling *Bmi1*-expressing stem cells situated at position +4 above the crypt base (Barker et al., 2007; Sangiorgi and Capecchi, 2008). In the small intestine, the stem cell markers *Sox-9* and *Hes1* are also expressed in actively cycling *Lgr5*$^+$ cells, while *Bmi*-1, *mTert*, *Hopx* and *Lrig1* are expressed in relatively quiescent stem cells, confirming the existence of more than one stem cell pool (Fre et al., 2011; Furuyama et al., 2011; Montgomery et al., 2011; Powell et al., 2012; Takeda et al., 2011). Moreover, *Lgr5*$^+$ cells are dispensable in the small intestine, with *Bmi1*$^+$ stem cells able to regenerate *Lgr5*$^+$ cells and their lineages (Tian et al., 2011).

The epithelial lining of the colon is also comprised of a single layer of columnar epithelial cells that are constantly renewed by a pool of committed stem cells. These colonic stem cells give rise to progeny that terminally differentiate into a number of lineages that include colonocytes, mucus-secreting goblet cells, and enteroendocrine cells. Most recent studies have suggested that colonic stem cells are located at the crypt base throughout the colon, and a number of markers for colon stem cells have been proposed, including Lgr5 (Barker et al., 2007), Lrig1 (Powell et al., 2012), Sox9 (Ramalingam et al., 2012), and EphB2 (Jung et al., 2011). Lgr5 has been the best studied, with in vivo lineage-tracing showing that Lgr5-expressing cells at the colonic crypt base are capable of self-renewal and able to differentiate into all three colonic lineages. In the colon, however, it has been more challenging to identify the stem cells that reside above the crypt base. *Bmi1*$^+$ cells, for example, do not exist in the colon. Thus, it is not known whether more than one distinct stem cell pool exists in the colon.

Tumors are postulated to arise from tissue stem or progenitor cells, but the relative contribution of different stem cell pools to tumorigenesis remains unknown (Barker et al., 2009). In addition, our current understanding of colon cancer is based on a model of clonal evolution, whereby early adenomas advance to invasive carcinomas through stepwise acquisition of mutations (Fearon and Vogelstein, 1990). In rapidly proliferating tissues such as the intestine or colon, however, this model of tumorigenesis implies that only stem cells are sufficiently long-lived to accumulate the requisite mutations. Indeed, the contribution of *Lgr5*$^+$ stem cells to intestinal tumorigenesis has been demonstrated by the formation of adenomas upon targeted mutation of the *Apc* gene specifically in *Lgr5*$^+$ cells (Barker et al., 2009). Nonetheless, the contribution of additional *Lgr5*-negative stem cells to the cellular origin of both colonic and intestinal cancer has not been clarified.

To determine if an *Lgr5*-negative stem cell contributes to colonic homeostasis and tumor initiation, we established a genetic fate-mapping system for labeling *keratin*-19 (*Krt19*) expressing progenitor/stem cells. Cytokeratins are a multigene family of intermediate filaments, critical in the maintenance of the cytoskeleton but expressed in different lineages within the epithelium (Moll R et al, Cell 1982). Cytokeratin 19 or Krt19 is the smallest known acid keratin (~40kDa), and is epithelial specific, found in a broad range of epithelial tissues. In the gastrointestinal tract, Krt19 expression is restricted to the proliferating compartments of the stomach, small intestine and colon, as well as the pancreatic ducts of the adult pancreas and the hepatobiliary ducts (Brembeck et al., 2001). *Krt19* is expressed in

the stem cell zone of the hair follicle (Brembeck et al., 2001; Lapouge et al., 2011; Means et al., 2008), is amplified in many solid tumors and, as we demonstrate here, is expressed near the presumptive progenitor/stem cell zone of both the colon and intestine. More specifically, we examined *Krt19* because it is expressed at position +4 extending up to the isthmus, thus allowing us to selectively label a population of cells that included transit amplifying cells, progenitors and long-lived stem cells, yet exclude rapidly cycling CBC *Lgr5*$^+$ stem cells.

We compared *Krt19*$^+$ cells above the crypt base to *Lgr5*$^+$ CBC cells with respect to their response to epithelial injury and cancer initiating ability. *Krt19*-expressing cells identify long-lived progenitors/stem cells distinct from *Lgr5*$^+$ cells, and additionally render *Lgr5*$^+$ stem cells dispensable in both the colon and intestine. Under conditional loss of the *Apc* gene, *Krt19*$^+$ stem cells also display cancer initiating ability, yet are functionally distinct from *Lgr5*$^+$ cancer initiating cells by their relative radioresistance.

Results

Krt19 transcript localizes to the stem cell zone above the crypt base and marks both colonic and intestinal stem cells

To localize *Krt19* mRNA and protein expression, we performed *in situ* hybridization for *Krt19* mRNA and immunofluorescence staining for Krt19 protein. *Krt19* RNA was completely absent from the colonic crypt base, and was detected primarily in the isthmus (i.e. area of crypt narrowing) that included cells extending down near the presumptive crypt progenitor/stem cell zone (Figure 1A, S1A). In contrast, *Krt19* protein showed minimal overlap with *Krt19* RNA, and was localized predominantly in differentiated cells (Figure S1B). Similarly, in the intestine *Krt19* RNA was detected primarily in the isthmus and not the intestinal crypt base (Figure 1B, S1B), while *Krt19* protein expression localized to differentiated cells of the intestinal villus (Figure S1D). We have previously reported a progenitor/stem cell marker in the stomach that similarly displayed a discrepancy in the pattern between RNA versus protein expression (Quante et al., 2010), so we sought to examine whether *Krt19* also marked a stem cell population. We developed a Krt19-BAC-mApple (*Krt19*-mApple) reporter mouse (Figure S1I) confirming that Krt19 gene expression was limited only to cells located well above the crypt base in both the colon (Figure 1C) and intestine (Figure 1D). Notably, the absence of both *Krt19* mRNA and protein expression from the crypt base (Figure 1A–D and S1A–H) afforded us the unique opportunity to selectively label and compare a progenitor/stem cell pool situated above the crypt base (position +4) to the well described *Lgr5*$^+$ CBC cells (Barker et al., 2007), and the more recently reported *Lrig1*$^+$ stem cells (Powell et al., 2012) found at the crypt base.

To identify an *Lgr5*-negative progenitor/stem cell pool in the colon, we established a genetic fate-mapping system for labeling *Krt19*. We generated a *Krt19*-BAC-*CreERT2* (*Krt19*-CreERT) transgenic line (Figure S1J–K) that was crossed to R26-LacZ (R26-LacZ) and ROSA26-mT/mG (R26-mT/mG) reporters in order to perform genetic lineage tracing experiments in homeostasis, inflammation and cancer. Shortly following tamoxifen induction, β-gal$^+$ cells were localized to the colonic crypt (Figure 1E) in a pattern identical to *Krt19*-expressing cells detected by *in situ* and *Krt19*-mApple$^+$ cells detected using a *Krt19*-mApple transgenic reporter mouse. Twenty-four (24) hours after tamoxifen,

recombination was evident in the colonic isthmus extending down to the +4 position, but distinctly above the crypt base (Fig. 1G and S2A). One week (1 wk) following tamoxifen, recombined cells derived from *Krt19*$^+$ cells extended downward to include *Lgr5*$^+$ cells at the colonic crypt base (Figure 1G, and S2A). Sixteen weeks (16 wk) post-induction, *Krt19*$^+$ cells traced all epithelial cell lineages in the colon (Figure 1G and S2A), and completely labeled glands were detected without any loss of labeling beyond 52 weeks (Figure 1G and S2A–D), consistent with *Krt19* labeling long-lived stem cells.

In vitro, two-photon florescence microscopy of colonic crypts isolated from *Krt19*-CreERT;R26-mT/mG mice 12 h after a single dose of tamoxifen also revealed recombination (GFP+) in a number of *Krt19*-expressing cells above the crypt base (Figure 1I–J; n=6, colon). These cells contained *bona fide* stem cells and gradually replaced all epithelial cells over 9–10 days (colon: Figure 1I–J).

Similarly, in the intestine, genetic lineage tracing experiments revealed that shortly following tamoxifen induction, Krt19 labeled β-gal$^+$ cells located clearly above the crypt base in the intestinal crypt (Figure 1K and S2E). These cells eventually traced all intestinal epithelial cell lineages, including *Lgr5*$^+$ cells at the crypt base (Figure 1K and S2E–F), and again, consistent with the labeling of long lived stem cells, we observed no loss of labeling beyond 52 weeks (Figure 1C–D). Furthermore, in intestinal enteroids grown *in vitro*, a few *Krt19*$^+$ cells above the crypt base could be detected 12h following tamoxifen (Figure S2G–I; n=4, intestine) and these cells expanded over 9–10 days to replace the entire crypt-villus column (Figure S2G–I). Single cell culture of *Krt19*-mApple$^+$ cells isolated from the intestine of *Krt19*-mApple reporter mice further confirmed the stem cell capacity of *Krt19*$^+$ cells (Figure S2J) at ~1% clonogenic efficiency compared to 5% for Lgr5-GFP$^+$ cells.

Krt19$^+$ potential stem cells above the crypt base are distinct from *Lgr5*$^+$ CBCs

To measure the overlap of *Krt19*$^+$ cells with *Lgr5*$^+$ cells, we performed *Krt19 in situ* hybridization on colonic (Figure 2A) tissues of *Lgr5*-EGFP-IRES-CreERT2 mice. We confirmed that *Krt19* mRNA expression was not detectable in CBC stem cells marked by *Lgr5*, and overlapped rarely with a very small subset of *Lgr5*-GFP positive cells located much higher in the colonic crypt (average position +7) (Figure 2C). Similarly, *Krt19* mRNA expression was not detectable in *Lgr5*$^+$ CBCs in the intestine (Figure 2B), and again overlapped rarely with a very small subset of *Lgr5*-GFP positive cells located much higher in the crypt (average position +7) (Figure 2C). The majority of *Krt19*$^+$ cells were also distinct from *Lgr5*$^+$ cells with respect to their proliferation status, as most *Lgr5*$^+$ cells were located immediately below the proliferation zone, whereas *Krt19*$^+$ cells predominated within the proliferation zone (~12% *Lgr5*$^+$/Ki67$^+$ versus ~50% *Krt19*$^+$/Ki67$^+$ cells) (Figure 2D–F and S3A–J). Importantly, when we generated *Krt19*-mApple;*Lgr5*-EGFP-IRES-CreERT2 dual reporter mice, *Krt19*-mApple$^+$/*Lgr5*-GFP$^+$ double positive cells were only detected in extremely rare cells located higher in the colonic crypt (Figure 2G) and comprised <0.05% of total epithelial cells and <6% of Lgr5-GFP$^+$ cells as detected by FACS (Figure 2I–J, S3K). Similarly, in the intestine, <0.01% of total epithelial cells, and <5% of Lgr5-GFP$^+$ cells were *Krt19*-mApple$^+$/*Lgr5*-GFP$^+$ double positive cells as determined by imaging

(Figure 2H) and FACS analysis (Figure 2J and S3K). Thus, *Krt19* and *Lgr5* identify largely distinct populations (Figure 2K), with only rare overlap near the +7 cell region.

Interestingly, RNA expression analysis revealed that the *Krt19*-mApple^{+}/*Lgr5*-GFP^{+} double positive intestinal cells displayed significant enrichment for the known "+4" intestinal stem cell markers *Bmi1*, *Hopx*, *Lrig1*, as well as the intestinal progenitor marker *Dll1* (Figure 2L), whereas *Lgr5*-negative *Krt19*-mApple^{+} cells showed relatively low or undetectable levels of both "+4" stem cell and progenitor markers (Figure 2L). Remarkably, despite the heterogeneity of *Krt19*$^{+}$ cells posing a potential confounding factor in this RNA expression analysis, we confirmed using microscopy that only rare *Krt19*$^{+}$/*Bmi1*$^{+}$ cells are detected in the crypts of *Krt19*-CreERT;ROSA26-Tomato mice crossed to *Bmi1*-GFP mice (Figure S3L).

Thus, given the infrequent overlap of *Krt19* and *Lgr5*, we sought to definitively distinguish between *Krt19*$^{+}$ versus Lgr5^{+} cells. We generated *Lgr5*-DTR-EGFP;*Krt19*-CreERT;R26-Tomato mice to conditionally ablate *Lgr5*$^{+}$ cells following administration of diphtheria toxin, as previously described (Tian et al., 2011). First, we confirmed at twenty-four hours following tamoxifen induction that *Krt19*-Tomato^{+} cells were located above the crypt base, and almost entirely distinct from *Lgr5*-GFP^{+} CBCs, (Figure 3A–B). Next, we administered diphtheria toxin (DT) three days prior to tamoxifen in order to ablate *Lgr5*$^{+}$ cells before the start of *Krt19* lineage tracing (Figure 3C). Interestingly, *Krt19*$^{+}$ colonic stem cells continued to lineage trace in the colon, and gave rise to new *Lgr5*-GFP^{+} cells when the diphtheria toxin was stopped (Figure 3D). Importantly, the efficiency of *Krt19*$^{+}$ cell lineage tracing was unchanged despite *Lgr5*$^{+}$ cell ablation effectively eliminating both the *Lgr5*-GFP^{+} CBCs, as well as the rare "+4" *Krt19*-mApple^{+}/*Lgr5*-GFP^{+} double positive cell populations (Figure 3E).

Similarly, *Krt19*$^{+}$ cells in the intestine continued to lineage trace and display resiliency in the face of *Lgr5*-GFP^{+} cell ablation (Figure 3D). From these data, we conclude that *Krt19*$^{+}$ lineage tracing in the intestine was not due to overlap with the *Dll1*$^{+}$ progenitor population for several reasons. First, *Dll1* RNA expression was predominantly detected within the rare "+4" *Krt19*-mApple^{+}/*Lgr5*-GFP^{+} double positive and *Lgr5*-GFP^{+} CBC populations, rather than *Krt19*-mApple^{+} cells. Moreover, *Dll1*$^{+}$ progenitors are reported to show no lineage tracing capacity when irradiated 2 weeks after tamoxifen (van Es et al., 2012), and additionally, are unable to form intestinal enteroids in the absence of Wnt3a (van Es et al., 2012). In contrast, *Krt19*$^{+}$ cells formed intestinal enteroids in the absence of Wnt3a (Figure S4A–C) and also showed lineage tracing capacity in vivo when irradiated 2 weeks after tamoxifen (Figure 4K–L).

Krt19^{+} lineage tracing capacity was not due to overlap with *Krt19*$^{+}$ transit amplifying (TA) cells. We used 5-fluorouracil (5-FU) to target the rapidly proliferating TA cell population as previously described (Doetsch et al., 1999; Stange et al., 2013), and confirmed that this treatment eliminated nearly all (> 95%) of the proliferating TA cells in both the colon and intestine (Figure 3F–H, S4D). *Krt19*$^{+}$ cells lineage traced with the same efficiency in both the colon and intestine regardless of TA cell ablation alone, or TA cell plus *Lgr5*$^{+}$ cell ablation (Figure 3J–I). Taken together, these data prove that *Krt19* identifies a novel *Lgr5*(−)

Krt19-expressing potential stem cell population in both the colon and intestine. Interestingly, *Krt19* and *Lgr5* additionally label distinct cell populations during development. Using a newly generated, constitutive *Krt19*-BAC-CRE transgenic mouse, we observed that *Krt19* marked the early gastrointestinal endoderm, raising the possibility that *Krt19* may also label a stem cell population in development (Figure S5A–G). This is in contrast to *Lgr5*-GFP^{+} cells which were first detected in the intestine as weakly GFP+ cells on post-natal day 5 (Figure S5H–I).

Krt19^{+} cells show relative radioresistance and are functionally distinct from *Lgr5*$^{+}$ stem cells and *Dll1*$^{+}$ progenitors

Radiation injury initiates intestinal stem cell division during epithelial repair (May et al., 2008; Yan et al., 2012), but *Lgr5*$^{+}$ stem cells have been proposed to be radiosensitive (van Es et al., 2012; Yan et al., 2012), whereas *Bmi1*$^{+}$ stem cells radioresistant (Yan et al., 2012). Thus, we sought to compare *Krt19*$^{+}$ versus *Lgr5*$^{+}$ stem cells with respect to their sensitivity to radiation. *Krt19*-CreERT;R26-LacZ and *Lgr5*-EGFP-IRES-CreERT2;R26-LacZ mice were irradiated (12 Gy) 24 h following tamoxifen labeling of each cell population (Figure 4A). When *Lgr5*-EGFP-IRES-CreERT2;R26-LacZ mice were irradiated 24 h after tamoxifen, absence of lineage tracing (Figure 4B and 4D and S6A) immediately following and in the early post radiation period confirmed that *Lgr5*$^{+}$ cells were radiosensitive (Yan et al., 2012). Consistent with *Lgr5*$^{+}$ cell radiosensitivity, we observed a loss of *Lgr5*-GFP expression immediately following radiation (Figure 4E). In contrast, radioresistant *Krt19*$^{+}$ cells continued to lineage trace in irradiated *Krt19*-CreERT;R26-LacZ mice (Figure 4C and S6B), and we detected an increase in contiguously labeled *Krt19*$^{+}$ crypts, consistent with crypt fission (Figure 4D) and stem cell expansion through symmetric division as previously described (Park et al., 1995). Moreover, the conclusion that radioresistance of *Krt19*$^{+}$ cells was due to the labeling of stem cells, rather than TA cells, was supported by our observations that targeting of TA cells with 5-FU prior to radiation did not alter the lineage tracing capacity of *Krt19*$^{+}$ cells (Figure 4G–H). *Krt19*$^{+}$ cells also showed longevity (> 18 months) well beyond the two week life-span of *Dll1*$^{+}$ progenitors and importantly, showed lineage tracing capacity even when irradiated 2 weeks following tamoxifen induction (Figure S6E–F).

To confirm our *in vivo* observations, we examined the effects of radiation on intestinal enteroid growth and stem cell function *in vitro* (Figure 4I). Following 10 Gy irradiation, intestinal enteroids from *Krt19*-mApple^{+}/*Lgr5*-GFP^{+}dual reporter mice showed a marked reduction in *Lgr5*-GFP^{+} stem cells associated with the loss of crypt budding suggestive of crypt injury (Figure 4I–J). In contrast, the same enteroids showed that *Krt19*-mApple expressing cells remained radioresistant and survived radiation injury. Indeed, during the regenerative state post radiation, newly budding crypts arose from radioresistant *Krt19*–mApple labeled cells (Figure 4J). These data again confirmed our *in vivo* observations that *Krt19*$^{+}$ cells show relative radioresistance when compared to *Lgr5*$^{+}$ stem cells.

Recently, it was shown that interconversion can occur between *Hopx*$^{+}$ and *Lgr5*$^{+}$ cells *in vitro* (Science 2012), and that *Dll1*$^{+}$ progenitors can also revert back to an *Lgr5*$^{+}$ state *in vitro* (van Es et al., 2012). Thus, we examined whether radiosensitive *Lgr5*$^{+}$ stem cells could

give rise to radioresistant stem cells *in vivo*. When we allowed for *Lgr5* lineage tracing to occur for up to two weeks prior to radiation (12Gy) exposure, we observed a significant increase in the number of contiguously labeled *Lgr5* traced SI crypts in *Lgr5*-EGFP-IRES-CreERT2;R26-LacZ mice after radiation (Figure 4K–N and S6C–D). Lineage tracing from *Lgr5*$^+$ cells was only observed when tamoxifen was administered at least two weeks prior to radiation, suggesting that *Lgr5*$^+$ cells can over time give rise to a radioresistant stem cell population such as *Krt19*$^+$ cells. We demonstrated that *Krt19*$^+$ cells give rise to *Lgr5*$^+$ cells (Figure 1G, 1K, S2A and S2E); thus, to our knowledge, this is the first *in vivo* evidence that stem cell interconversion readily occurs between radioresistant (*Krt19*$^+$) and radiosensitive (*Lgr5*$^+$) states.

Radioresistant *Krt19*$^+$ cancer initiating cells are functionally distinct from *Lgr5*$^+$ cells

The contribution of *Lgr5*$^+$ stem cells to early tumor development has previously been demonstrated by the formation of intestinal adenomas upon targeted mutation of the *Apc* gene in this lineage (5). However, the contribution of additional stem cell pools to the origin of cancer remains unknown. To determine whether *Krt19*$^+$ cells can also function as cancer initiating cells in the colon and intestine, we generated *Krt19*-CreERT;R26-LacZ;Apc$^{F/F}$ mice in which conditional expression of a truncated form of *Apc* occurs in *Krt19*$^+$ cells following tamoxifen induction. Analogous to *Lgr5*$^+$ stem cells, *Krt19*$^+$ cells initiated intestinal tumorigenesis following Apc deletion, resulting in rapid mortality (Figure 5A). To functionally distinguish between *Krt19*$^+$ and *Lgr5*$^+$ cancer-initiating cells, however, we further compared the susceptibility of these two stem cell pools to radiation injury. Interestingly, when irradiated 24h after tamoxifen, *Lgr5*-EGFP-IRES-CreERT2;R26-LacZ;Apc$^{F/F}$ mice showed no mortality (Figure 5B) and normal non-lineage traced colon and intestine (Figure 5C), whereas similarly treated *Krt19*-CreERT;R26-LacZ;Apc$^{F/F}$ mice continued to display rapid mortality (Figure 5B) from numerous lineage traced colonic and intestinal tumors (Figure 5D). Taken together, these observations provide evidence that *Krt19*$^+$ stem cells are cancer initiating cells distinct from *Lgr5*$^+$ cells.

Furthermore, when crypts from *Krt19*-CreERT; R26-mT/mG;Apc$^{F/F}$ mice were cultured *in vitro* 24 h after tamoxifen, recombined *Apc* floxed *Krt19*$^+$ cells appeared as GFP$^+$ spheroid structures (Figure 5E–F), which were easily distinguishable from non-recombined crypts that remained Tomato$^+$ and formed normal budding crypt structures. Consistent with our *in vivo* observations, following *in vitro* irradiation (10 Gy), *Apc* floxed *Krt19*$^+$ spheroids were radioresistant with no change in growth, and non-recombined *Apc* wild-type crypts showed radiosensitivity only within the budding crypts that contain *Lgr5*$^+$ stem cells (Figure 5G–I). Post-radiation, there was neither *in vitro* nor *in vivo Lgr5* mRNA expression, while *Krt19* mRNA actually increased (Figure 5J and 6A). Thus, radiosensitive *Lgr5*$^+$ stem cells are dispensable in both normal and *Apc* mutated crypts. Similarly, in *Apc* floxed tumors of *Lgr5*-EGFP-IRES-CreERT2;R26-LacZ;Apc$^{F/F}$ mice, we detected reduced *Lgr5*-GFP$^+$ cells, but unchanged *Krt19* protein positive cells 24 h post radiation (Figure 6B–C).

When we additionally performed DT ablation of *Lgr5*$^+$ cancer stem cells in crypts from *Lgr5*-DTR-EGFP;*Krt19*-CreERT;R26-LacZ;Apc$^{F/F}$ mice, we observed continued growth of many, but not all, *Krt19*$^+$ *Apc* floxed enteroids (Figure 6D–F). We confirmed the efficacy of

DT ablation of *Lgr5*$^+$ cells by the absence of *Lgr5* mRNA expression (Figure 6G), which again was associated with a corresponding increase in *Krt19* mRNA expression (Figure 6G). Importantly, *Krt19*$^+$ *Apc* floxed enteroids could also be maintained in culture in the absence of R-spondin, and were completely unaffected even by *Lgr5*$^+$ cell ablation in this setting (Figure 6H–I). These data prove, for the first time, that *Krt19*$^+$ cell derived *Apc* floxed enteroids are heterogeneous, with *Lgr5*$^+$ cancer stem cells being completely dispensable in these enteroids (Figure 6I–J).

Discussion

In contrast to the intestine, the paucity of stem cell markers in the colon has hampered our ability to identify and adequately characterize *Lgr5*-negative stem cell pools in normal and neoplastic colonic crypts. Here, we show that *Krt19*-expressing cells, extending from the +4 position to the crypt isthmus, include unique long-lived stem cells that are distinct from *Lgr5*$^+$ CBCs. The distinct nature of *Krt19*$^+$ versus *Lgr5*$^+$ stem cells was confirmed by the observation that *Krt19*$^+$ cells continue to lineage trace crypts despite ablation of *Lgr5*$^+$ stem cells in both the colon and intestine. *Krt19*$^+$ cells actively contribute to normal epithelial maintenance and are also clearly functionally distinct from *Lgr5*$^+$ stem cells by their relative radioresistance. The radioresistance of *Krt19*$^+$ cells holds true not only in the colon, but also in the intestine. Recognizing that *Krt19*-expressing cells comprise a heterogeneous population that also includes progenitor and TA cells, we confirmed that the differences in radiation response were nonetheless attributable to *Krt19*$^+$ stem cells. Indeed, the combination of TA cell targeting by 5-FU and DT ablation of *Lgr5*$^+$ cells confirmed that a unique population of *Krt19*$^+$ stem cells continue to lineage trace and expand following radiation injury. Notably, in the intestine, it has been shown that *Dll1*$^+$ progenitors and *Bmi1*$^+$ stem cells are radioresistant (van Es et al., 2012; Yan et al., 2012) while *Lgr5*$^+$ stem cells are radiosensitive. Interestingly, our observations regarding *Krt19*$^+$ cell radioresistance now extend these findings to the colon, where *Bmi1*$^+$ and *Dll1*$^+$ cells are not found (Sangiorgi and Capecchi, 2008; van Es et al., 2012). Moreover, *Krt19*$^+$ cells lineage trace independent of *Lgr5*$^+$ cells following radiation injury, as *Lgr5*$^+$ stem cells are radiosensitive when irradiated 24 h following tamoxifen induction. Taken together with the recent observations of *Metcalfe et al*., the rapid regeneration of *Lgr5*$^+$ cells in the immediate post radiation period is essential for epithelial repair and likely to occur from a radioresistant *Krt19*$^+$ population (Metcalfe et al., 2014). Thus, long-lived radioresistant *Krt19*$^+$ cells are functionally distinct from radiosensitive *Lgr5*$^+$ CBCs in both the colon and intestine.

Recent work by Takeda and colleagues (Takeda et al., 2011) suggested that interconversion between two or more stem cell pools occurs in enteroid cultures. Here, we demonstrate that *Krt19*$^+$ stem cells give rise to *Lgr5*$^+$ CBCs in both the colon and intestine, and that the reverse is also true. That is, radiosensitive *Lgr5*$^+$ stem cells give rise to *Krt19*$^+$ radioresistant cells, given enough time to interconvert following tamoxifen. Therefore, although previously speculated to be true, we provide the first *in vivo* evidence that *Lgr5*$^+$ cells can indeed give rise to a radioresistant stem cell population (Figure 4 and S6).

Although the colon was the predominant focus of the current study, the potential overlap of *Krt19* with other +4 intestinal stem cell markers or *Dll1*$^+$ progenitors raises the possibility

that some of our observations in the intestine could be attributed to overlap with these cell populations. It is important to note, however, that intestinal *Krt19*$^+$ cells are long-lived, survive well beyond 18 months, and show lineage tracing capacity even when irradiated 2 weeks following tamoxifen induction. This is true, not only in the colon, but also in the intestine, where this is in sharp contrast to intestinal *Dll1*$^+$ progenitors that are short-lived and do not display any lineage tracing capacity when irradiated beyond 24h following tamoxifen (van Es et al., 2012). Moreover, *Krt19*$^+$ cells remained capable of sustaining intestinal enteroids *in vitro*, despite ablation of *Lgr5*$^+$ stem cells and the absence of Wnt3a (a factor recently shown to be essential for *Dll1*$^+$ progenitor reversion to stem cells). Furthermore, our RNA expression analysis revealed that the overlap of *Krt19* with the various +4 intestinal stem cell markers, as well as *Dll1*, was only true of rare *Krt19*$^+$/*Lgr5*$^+$ double positive cells above the CBCs, yet DT ablation of all *Lgr5*$^+$ cells including this overlapping population had no effect on *Krt19*$^+$ stem cell lineage tracing activity. Taken together, these data prove that overlap with *Dll1*$^+$ progenitors and *Bmi1*$^+$ stem cells cannot solely explain our observations regarding radioresistance of *Krt19*$^+$ cells in the intestine.

Ritsma and colleagues recently suggested that *Lgr5*$^+$ cells display heterogeneity based on their “border” versus “central” position within the intestinal crypt (Ritsma et al., 2014). Our own observations that a rare subset of *Lgr5*$^+$ cells expresses *Krt19*, while the majority of *Lgr5*$^+$ cells do not, supports the premise of heterogeneity among *Lgr5*$^+$ cells, and additionally, leads one to speculate whether *Krt19*-mApple$^+$/*Lgr5*-GFP$^+$ double positive cells identify a unique subset of *Lgr5*$^+$ cells with “potential” stem cell activity as previously described (Kozar et al., 2013).

Conditional expression of a truncated form of *Apc* additionally confirmed that *Krt19*$^+$ cells include a population of cancer initiating cells. That cancer initiation in *Lgr5*-EGFP-IRES-CreERT2;R26-LacZ;Apc$^{F/F}$ mice was completely suppressed in the colon as well as the intestine by high dose radiation 24h following tamoxifen confirmed that *Lgr5*$^+$ cancer initiating cells were radiosensitive. In contrast, similarly treated *Krt19*-CreERT;R26-LacZ;Apc$^{F/F}$ mice developed many colonic and intestinal tumors despite irradiation, again demonstrating the functional distinction of *Krt19*$^+$ versus *Lgr5*$^+$ cancer initiating cells. Thus, we provide the first definitive evidence of an *Krt19*$^+$/*Lgr5*(−) radioresistant cancer initiating cell population in both the colon and intestine. In view of the high prevalence of colon cancer and inflammatory conditions affecting the colon, the identification of colonic *Krt19*$^+$/*Lgr5*(−) cancer initiating stem cells is highly relevant to our understanding and treatment of human disease. Additionally, we now demonstrate that *Lgr5*$^+$ cancer stem cells are dispensable in *Apc* floxed tumors, particularly in R-spondin independent conditions. In view of the recent findings that R-spondin fusion proteins activate Wnt signaling in a subset of human colorectal tumors, our observations may have important implications for *Lgr5*$^+$ cell targeted therapy in subsets of colorectal cancer patients (Seshagiri et al. 2012).

In summary, we identify a novel population of colonic *Krt19*$^+$ cells that give rise to *Lgr5*$^+$ CBC cells. Radioresistant *Krt19*$^+$ cells located above the crypt base can initiate cancer and are functionally distinct from radiosensitive *Lgr5*$^+$ CBCs. These findings have important clinical relevance for future cancer therapy targeting colonic stem cell populations.

Materials & Methods

Generation of *Krt19*-CreERT2 transgenic mice

For BAC recombineering, the K19 containing BAC clone (BAC RP-23-24N13) was transformed into SW105 competent cells and a *Krt19*-BAC-CreERT2 construct generated by BAC recombineering. See Supplementary Information for further details.

Lineage tracing analysis and assessment and immunofluorescence

Intestinal and colonic tissues were prepared as swiss rolls and sections fixed with 4% paraformaldehyde and β-galactosidase labeling assessed by X-gal staining of frozen sections taken from R26rLacZ mice. Mice were sacrificed at various time points post tamoxifen and analyzed at the time points specified. We similarly analyzed tissues from R26-mT/mG reporter mice for EGFP positive cells and their progeny at various time points post tamoxifen. Further details are outlined in the supplementary methods. For immunostaining, we performed staining of frozen sections with antibodies according to the methods detailed in the Supplementary Information.

Flow Cytometry

Single-cell suspensions were stained with antibodies and analyzed on FACS Calibur, Aria III (BD) or Gallios (Beckman Coulter). FlowJo software (Ashland) was used for data analysis. Detailed methods and antibodies are described in the Supplemental Information.

In situ hybridization

Using a cRNA probe constructed and labeled for *Krt19*, paraformaldehyde fixed SI and colonic tissues were hybridized with the probe. Detailed methods and antibodies are described in the Supplemental Information.

Statistical analysis

Statistical analysis was performed with Student’s t-test or Mann-Whitney when comparing two groups or standard ANOVA analysis with Bonferri correction. Values of * ($P<0.05$) and ** ($P<0.01$) were considered statistically significant.

Enteroid in vitro cultures

Intestinal or colonic glands units were isolated from mouse as previously described by Bjerknes and Cheng with some modifications, and cultured in the presence of EGF 50 ng/ml (Invitrogen), mNoggin 100 ng/ml (Peprotech), and R-Spondin 1 ug/ml as previously described (Sato et al., 2009). Detailed protocols are described in the Supplemental Information.

Supplementary Material

Refer to Web version on PubMed Central for supplementary material.

Acknowledgments

The authors thank the members of the Irving Cancer Research Center Core Microscopy Core Facility for their technical assistance. We also thank Genentech for their generosity in providing the *Lgr5*-GFP-DTR knock-in mice used for this study. The authors also recognize the technical assistance of Yagnesh Tailor, Karan Nagar, Chintan Kapadia and Kelly Betz. Dr. Samuel Asfaha is supported by a CIHR Clinician Scientist Phase I Award and AHFMR Clinical Fellowship Award. This work was supported by NIH UO1 DK103155, NIH R37 DK052778 and NIH RO1 DK097016 to Timothy C. Wang, and NIH R01 DK056645, Hansen Foundation and National Colon Cancer Research Alliance (AKR) and NIH P30 DK 050306 (AKR) and its Mouse Core Facility.

References

Barker N, Ridgway RA, van Es JH, van de Wetering M, Begthel H, van den Born M, Danenberg E, Clarke AR, Sansom OJ, Clevers H. Crypt stem cells as the cells-of-origin of intestinal cancer. Nature. 2009; 457:608–611. [PubMed: 19092804]

Barker N, van Es JH, Kuipers J, Kujala P, van den Born M, Cozijnsen M, Haegebarth A, Korving J, Begthel H, Peters PJ, et al. Identification of stem cells in small intestine and colon by marker gene Lgr5. Nature. 2007; 449:1003–1007. [PubMed: 17934449]

Brembeck FH, Moffett J, Wang TC, Rustgi AK. The keratin 19 promoter is potent for cell-specific targeting of genes in transgenic mice. Gastroenterology. 2001; 120:1720–1728. [PubMed: 11375953]

Doetsch F, Caille I, Lim DA, Garcia-Verdugo JM, Alvarez-Buylla A. Subventricular zone astrocytes are neural stem cells in the adult mammalian brain. Cell. 1999; 97:703–716. [PubMed: 10380923]

Fearon ER, Vogelstein B. A genetic model for colorectal tumorigenesis. Cell. 1990; 61:759–767. [PubMed: 2188735]

Fre S, Hannezo E, Sale S, Huyghe M, Lafkas D, Kissel H, Louvi A, Greve J, Louvard D, Artavanis-Tsakonas S. Notch lineages and activity in intestinal stem cells determined by a new set of knock-in mice. PloS one. 2011; 6:e25785. [PubMed: 21991352]

Furuyama K, Kawaguchi Y, Akiyama H, Horiguchi M, Kodama S, Kuhara T, Hosokawa S, Elbahrawy A, Soeda T, Koizumi M, et al. Continuous cell supply from a Sox9-expressing progenitor zone in adult liver, exocrine pancreas and intestine. Nature genetics. 2011; 43:34–41. [PubMed: 21113154]

Jung P, Sato T, Merlos-Suarez A, Barriga FM, Iglesias M, Rossell D, Auer H, Gallardo M, Blasco MA, Sancho E, et al. Isolation and in vitro expansion of human colonic stem cells. Nature medicine. 2011; 17:1225–1227.

Kozar S, Morrissey E, Nicholson AM, van der Heijden M, Zecchini HI, Kemp R, Tavare S, Vermeulen L, Winton DJ. Continuous clonal labeling reveals small numbers of functional stem cells in intestinal crypts and adenomas. Cell stem cell. 2013; 13:626–633. [PubMed: 24035355]

Lapouge G, Youssef KK, Vokaer B, Achouri Y, Michaux C, Sotiropoulou PA, Blanpain C. Identifying the cellular origin of squamous skin tumors. Proceedings of the National Academy of Sciences of the United States of America. 2011; 108:7431–7436. [PubMed: 21502497]

Li L, Clevers H. Coexistence of quiescent and active adult stem cells in mammals. Science. 2010; 327:542–545. [PubMed: 20110496]

May R, Riehl TE, Hunt C, Sureban SM, Anant S, Houchen CW. Identification of a novel putative gastrointestinal stem cell and adenoma stem cell marker, doublecortin and CaM kinase-like-1, following radiation injury and in adenomatous polyposis coli/multiple intestinal neoplasia mice. Stem cells. 2008; 26:630–637. [PubMed: 18055444]

Means AL, Xu Y, Zhao A, Ray KC, Gu G. A CK19(CreERT) knockin mouse line allows for conditional DNA recombination in epithelial cells in multiple endodermal organs. Genesis. 2008; 46:318–323. [PubMed: 18543299]

Metcalfe C, Kljavin NM, Ybarra R, de Sauvage FJ. Lgr5+ stem cells are indispensable for radiation-induced intestinal regeneration. Cell stem cell. 2014; 14:149–159. [PubMed: 24332836]

Montgomery RK, Carlone DL, Richmond CA, Farilla L, Kranendonk ME, Henderson DE, Baffour-Awuah NY, Ambruzs DM, Fogli LK, Algra S, et al. Mouse telomerase reverse transcriptase (mTert) expression marks slowly cycling intestinal stem cells. Proceedings of the National Academy of Sciences of the United States of America. 2011; 108:179–184. [PubMed: 21173232]

Park HS, Goodlad RA, Wright NA. Crypt fission in the small intestine and colon. A mechanism for the emergence of G6PD locus-mutated crypts after treatment with mutagens. The American journal of pathology. 1995; 147:1416–1427. [PubMed: 7485404]

Powell AE, Wang Y, Li Y, Poulin EJ, Means AL, Washington MK, Higginbotham JN, Juchheim A, Prasad N, Levy SE, et al. The pan-ErbB negative regulator Lrig1 is an intestinal stem cell marker that functions as a tumor suppressor. Cell. 2012; 149:146–158. [PubMed: 22464327]

Quante M, Marrache F, Goldenring JR, Wang TC. TFF2 mRNA transcript expression marks a gland progenitor cell of the gastric oxyntic mucosa. Gastroenterology. 2010; 139:2018–2027. e2012. [PubMed: 20708616]

Ramalingam S, Daughtridge GW, Johnston MJ, Gracz AD, Magness ST. Distinct levels of Sox9 expression mark colon epithelial stem cells that form colonoids in culture. American journal of physiology Gastrointestinal and liver physiology. 2012; 302:G10–20. [PubMed: 21995959]

Ritsma L, Ellenbroek SI, Zomer A, Snippert HJ, de Sauvage FJ, Simons BD, Clevers H, van Rheenen J. Intestinal crypt homeostasis revealed at single-stem-cell level by in vivo live imaging. Nature. 2014; 507:362–365. [PubMed: 24531760]

Sangiorgi E, Capecchi MR. Bmi1 is expressed in vivo in intestinal stem cells. Nature genetics. 2008; 40:915–920. [PubMed: 18536716]

Sato T, Vries RG, Snippert HJ, van de Wetering M, Barker N, Stange DE, van Es JH, Abo A, Kujala P, Peters PJ, et al. Single Lgr5 stem cells build crypt-villus structures in vitro without a mesenchymal niche. Nature. 2009; 459:262–265. [PubMed: 19329995]

Stange DE, Koo BK, Huch M, Sibbel G, Basak O, Lyubimova A, Kujala P, Bartfeld S, Koster J, Geahlen JH, et al. Differentiated Troy+ chief cells act as reserve stem cells to generate all lineages of the stomach epithelium. Cell. 2013; 155:357–368. [PubMed: 24120136]

Takeda N, Jain R, LeBoeuf MR, Wang Q, Lu MM, Epstein JA. Interconversion between intestinal stem cell populations in distinct niches. Science. 2011; 334:1420–1424. [PubMed: 22075725]

Tian H, Biehs B, Warming S, Leong KG, Rangell L, Klein OD, de Sauvage FJ. A reserve stem cell population in small intestine renders Lgr5-positive cells dispensable. Nature. 2011; 478:255–259. [PubMed: 21927002]

van Es JH, Sato T, van de Wetering M, Lyubimova A, Nee AN, Gregorieff A, Sasaki N, Zeinstra L, van den Born M, Korving J, et al. Dll1+ secretory progenitor cells revert to stem cells upon crypt damage. Nature cell biology. 2012; 14:1099–1104.

Yan KS, Chia LA, Li X, Ootani A, Su J, Lee JY, Su N, Luo Y, Heilshorn SC, Amieva MR, et al. The intestinal stem cell markers Bmi1 and Lgr5 identify two functionally distinct populations. Proceedings of the National Academy of Sciences of the United States of America. 2012; 109:466–471. [PubMed: 22190486]

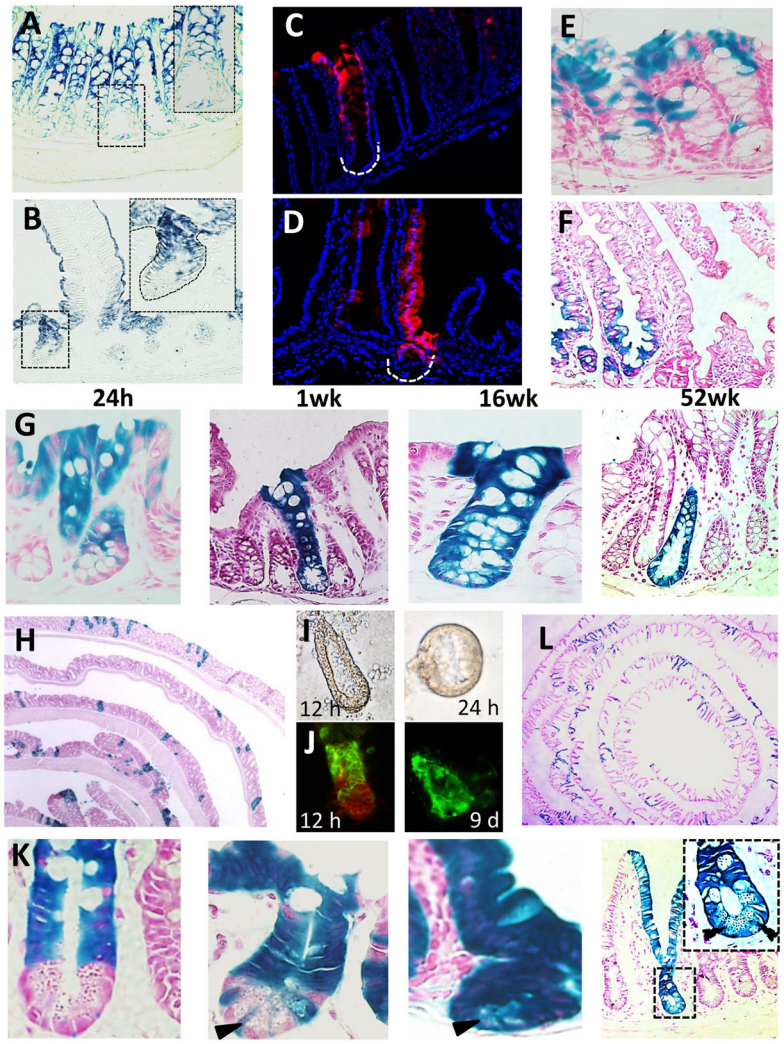

Figure 1. Krt19 mRNA localizes to the colonic and intestinal stem cell zone and marks long-lived stem cells

Krt19 mRNA is expressed in the isthmus extending down to the +4 position of the colonic (A) and (B) intestinal crypt. High magnification images of the crypt base are shown as insets. *Krt19*-mApple^{+} cells in the colon (C) and small intestine (D) of *Krt19-mApple* reporter mice show expression similar to in situ. 24 h post tamoxifen, β-gal^{+} colonic (E) and intestinal (F) crypts in *Krt19*-CreERT;R26RLacZ mice also show expression identical to in situ. Lineage tracing in the colon (G) of *Krt19*-CreERT;R26RLacZ mice. High magnification images of the crypt base are shown at 24 hours and 52 weeks following tamoxifen (6 mg p.o.). Low magnification images of lineage tracing in the colon (H) of *Krt19*-CreERT;R26RLacZ 26 weeks following tamoxifen (n ≥ 7 per group). Bright-field (6 and 24 hours after culture) (I) and 2-photon images (24 hours and 9 days following tamoxifen (6 mg p.o.)) (J) of colonic crypts from *Krt19*-CreERT; R26-mT/mG mice (n ≥ 4 per group) cultured *in vitro*. Lineage tracing in the intestine (K) in *Krt19*-CreERT/ R26RLacZ mice with high magnification images of the crypt base shown at 24 hours to 52 weeks following tamoxifen (6 mg p.o.). Note black arrows that show Krt19-derived CBCs at 7 days and Paneth cells at 16 and 52 weeks. Low magnification images of lineage tracing in

the intestine (L) of *Krt19*-CreERT/R26RLacZ 26 weeks following tamoxifen (n ≥ 7 per group). See also Figure S1 and S2.

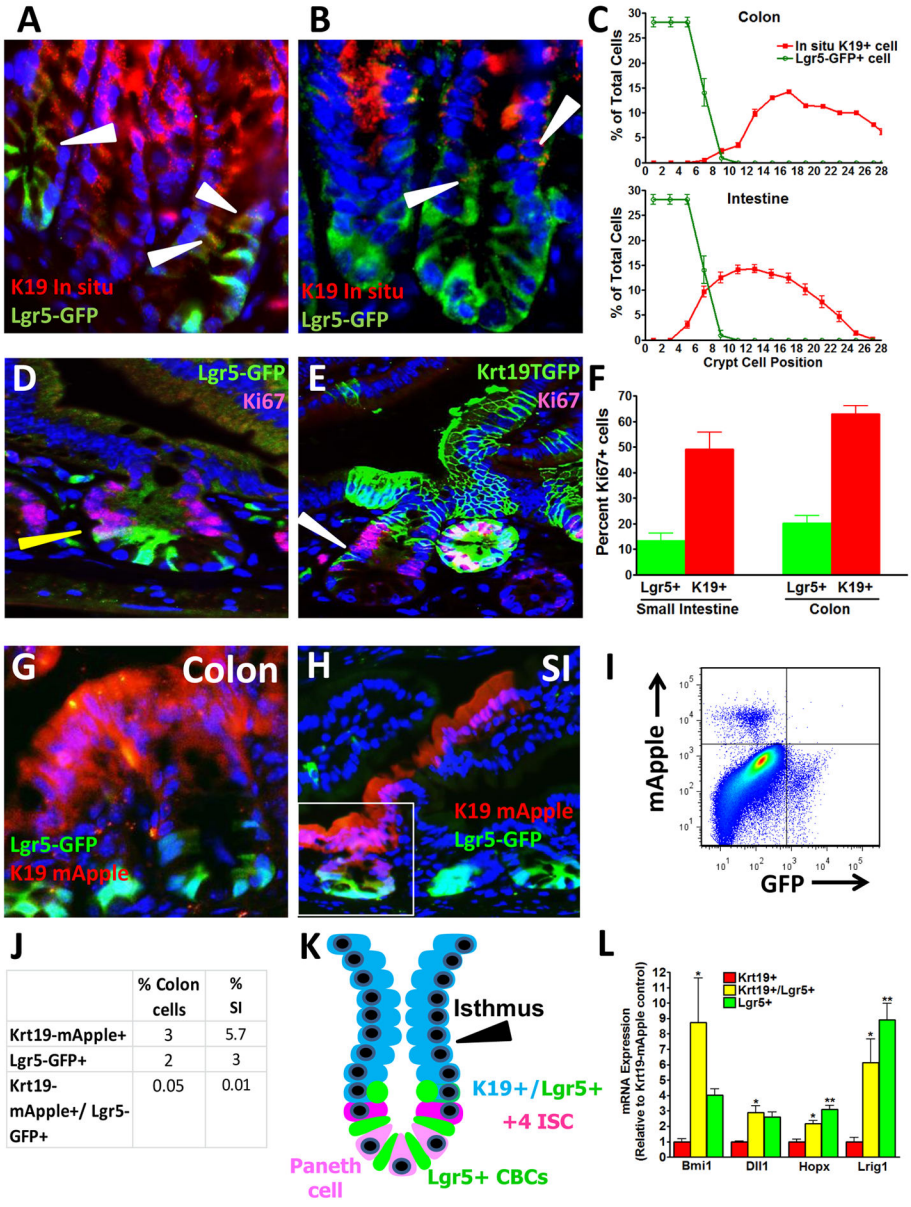

	% Colon cells	% SI
Krt19-mApple+	3	5.7
Lgr5-GFP+	2	3
Krt19-mApple+/ Lgr5-GFP+	0.05	0.01

Figure 2. *Krt19*$^+$ cells are located above *Lgr5*$^+$ crypt base columnar cells in the colon and intestine

Colocalization of *Krt19* mRNA expressing cells (red) detected by *in situ* and Lgr5-GFP$^+$ cells (green) in the colon (A) and small intestine (B) of *Lgr5*-EGFP-IRES-CreERT2 mice. White arrows denote double positive cells. (C) Average cell position of *Krt19* mRNA expressing (red) and *Lgr5*-EGFP$^+$ (green) cells within the colonic (top panel) and intestinal (bottom panel) crypt. Colocalization of Ki67 and *Lgr5*-EGFP$^+$ cells (D) versus Ki67 and *Krt19*-EGFP$^+$ cells 12 h after tamoxifen (E) in *Lgr5*-EGFP-IRES-CreERT2 or *Krt19*-CreERT;ROSA26-mG/mT mice, respectively. Yellow arrow shows a rare double positive (Ki67$^+$, Lgr5-GFP$^+$) cells and white arrow shows a rare Krt19$^+$, Ki67$^-$ cells. Quantification of double positive Ki67$^+$Krt19$^+$ cells (red bars) versus Ki67$^+$Lgr5-GFP$^+$ cells (green bars) (F). Representative images of the colon (G) and SI (H) of *Krt19*-mApple;*Lgr5*-EGFP-IRES-

CreERT2 dual reporter mice showing no overlap of *Krt19*-mApple^{+} and *Lgr5*-GFP^{+} cells in the colon and rare *Krt19*-mApple^{+}/*Lgr5*-GFP^{+} double positive cells higher in the crypt of the SI. FACS plot (I) and quantification (J) of colonic and intestinal *Krt19*-mApple^{+} and *Lgr5*-GFP^{+} positive cells from *Krt19*-mApple;*Lgr5*-EGFP-IRES-CreERT2 mice. Schematic diagram of the intestinal crypt demonstrating the location of *Krt19*-expressing cells in relation to *Lgr5*$^{+}$ crypt based columnar cells (K). mRNA expression levels of + 4 stem cell (*BMi1*, *Hopx* and *Lrig1*) and progenitor (*Dll1*) markers among *Krt19*-mApple^{+}, *Lgr5*-GFP^{+} and *Krt19*-mApple^{+}/*Lgr5*-GFP^{+} double positive cell populations (L). See also Figure S3.

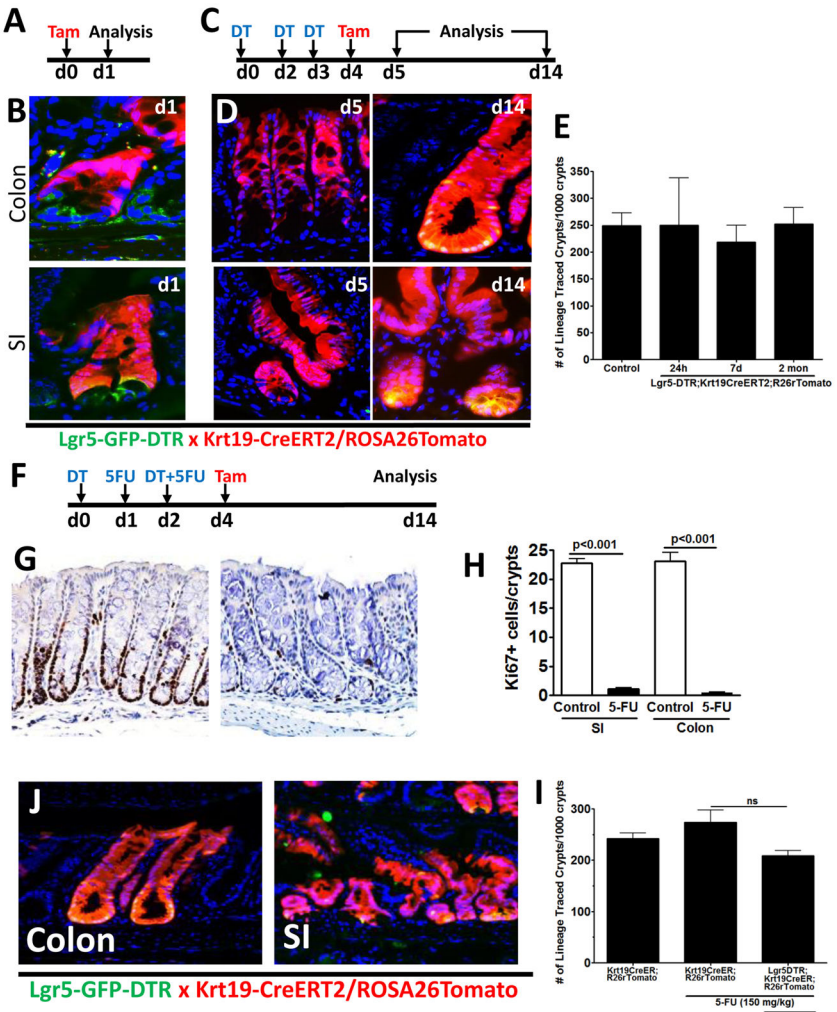

Figure 3. *Krt19*$^+$ stem cells render *Lgr5*$^+$ stem cells dispensable in the colon and small intestine

Tamoxifen protocol (A) used to analyze *Krt19*$^+$ and *Lgr5*$^+$ cells in *Lgr5*-DTR-EGFP;*Krt19*-CreERT/R26RTomato mice 24h post tamoxifen. Images of the colon and SI 24h post tamoxifen are shown (B). Diphtheria toxin (DT) ablation regimen (C) used in *Lgr5*-DTR-EGFP;*Krt19*-CreERT/R26RTomato mice showing *Krt19*$^+$ stem cells (red) render *Lgr5*$^+$ cells (green) dispensable in the colon and SI (D). Quantification of *Krt19*$^+$ stem cell lineage tracing efficiency in the presence or absence of *Lgr5*$^+$ stem cells (E) is shown. DT induced *Lgr5*$^+$ cells ablation and 5-FU induced transit amplifying (TA) cell ablation regimen (F) used in *Lgr5*-DTR-EGFP;*Krt19*-CreERT/R26RTomato mice. (G) Representative high power view of Ki67$^+$ cells in the colon of control (left) versus 5-FU treated (right) mice. Quantification of Ki67$^+$ cells in the colon or intestine of control versus 5-FU treated mice (H). *Krt19*$^+$ stem cells (red) render *Lgr5*$^+$ cells (green) dispensable in the colon and SI (J) in spite of 5-FU ablation of TA cells. Quantification of *Krt19*$^+$ stem cell lineage tracing efficiency in the presence or absence of *DT* and/or 5-FU stem cells (I) is shown ($n \geq 6$ per group). See also Figure S4 and S5.

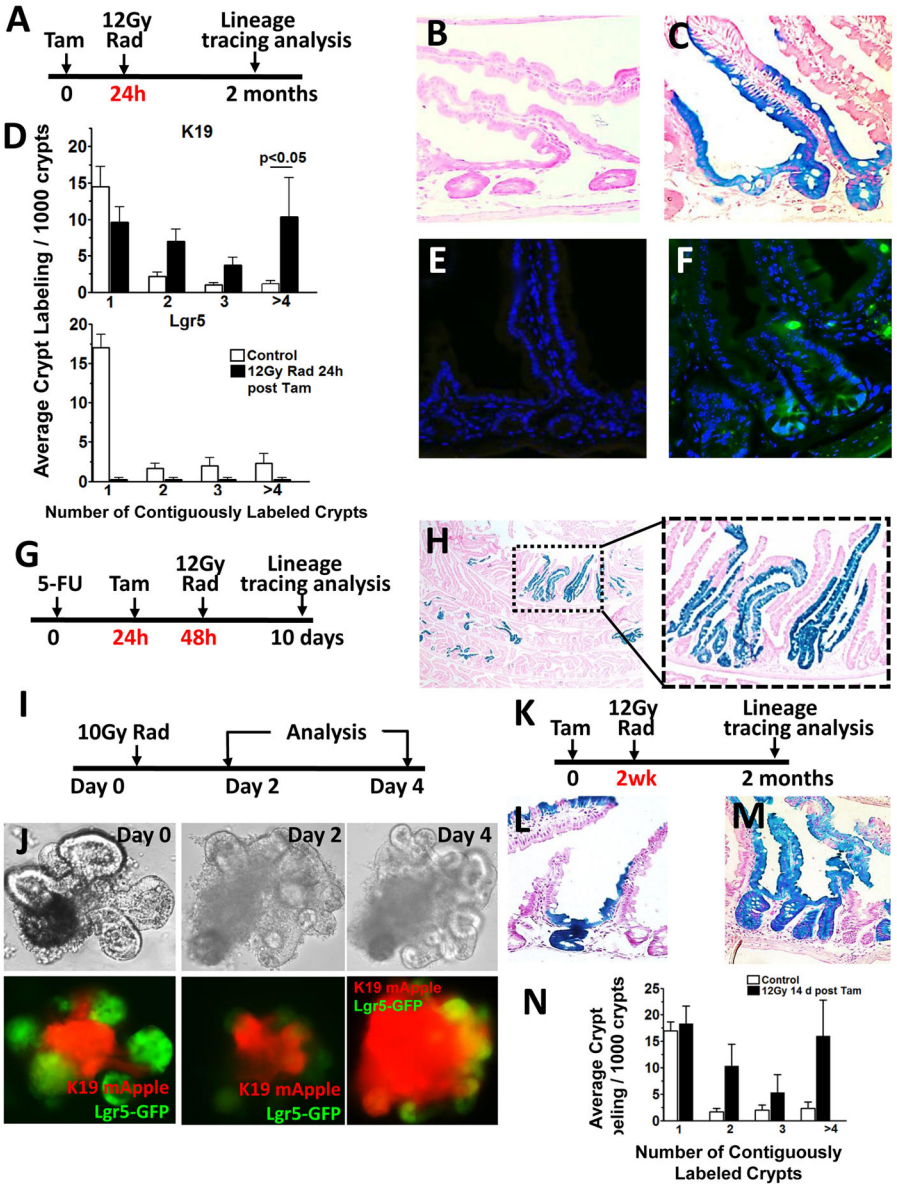

Figure 4. *Krt19*$^+$ cells expand in response to injury and display relative radioresistance compared to *Lgr5*$^+$ stem cells

To examine the radiosensitivity of *Krt19*$^+$ and *Lgr5*$^+$ stem cells, mice were irradiated 24 h after tamoxifen and lineage tracing examined 2 months following tamoxifen (A). Representative β-gal$^+$ intestinal crypts in *Lgr5*-EGFP-IRES-CreERT2;R26RLacZ (B) versus *Krt19-CreERT*;R26RLacZ (C) mice irradiated (12 Gy) 24 h post tamoxifen. Quantification of contiguously labeled β-gal$^+$ *Krt19* (top) versus *Lgr5* (bottom) labeled crypts following irradiation 24h after tamoxifen (D). Representative small intestinal crypt-villus image of *Lgr5*-EGFP-IRES-CreERT2;R26RLacZ mice following high dose radiation exposure demonstrating the disappearance of Lgr5-EGFP$^+$ crypt based columnar cells 24 h following irradiation (E) and re-emergence of EGFP$^+$ CBCs 7 days following irradiation (F). *In vivo* 5-FU (150 mg/kg) protocol used to examine the effects of TA cell ablation on *Krt19*$^+$ stem cell lineage tracing (G). Representative low (left) and high (right) power images of *Krt19*$^+$ cell

lineage tracing in *Krt19*-CreERT;R26RLacZ mice treated with 5-FU and examined 8 d post radiation (H). *In vitro* radiation protocol used to examine the effects of radiation injury on intestinal *Krt19* and *Lgr5* stem cell populations (I). Bright-field (top) and fluorescent (bottom) images of intestinal enteroids from *Krt19*-mApple^{+}/*Lgr5*-GFP^{+} double transgenic mice cultured *in vitro* pre and post radiation (10Gy) (J). Radiation protocol used to examine *Lgr5* derived lineage tracing in *Lgr5*-EGFP-IRES-CreERT2/R26RLacZ mice two weeks after tamoxifen (K). β-gal^{+} intestinal crypts from control (L) versus irradiated (M) *Lgr5*-EGFP-IRES-CreERT2;R26RLacZ mice. Quantification of contiguously labeled β-gal^{+} *Lgr5* labeled crypts following irradiation 2 weeks after tamoxifen (N); ($n \geq 5$ per group). See also Figure S6.

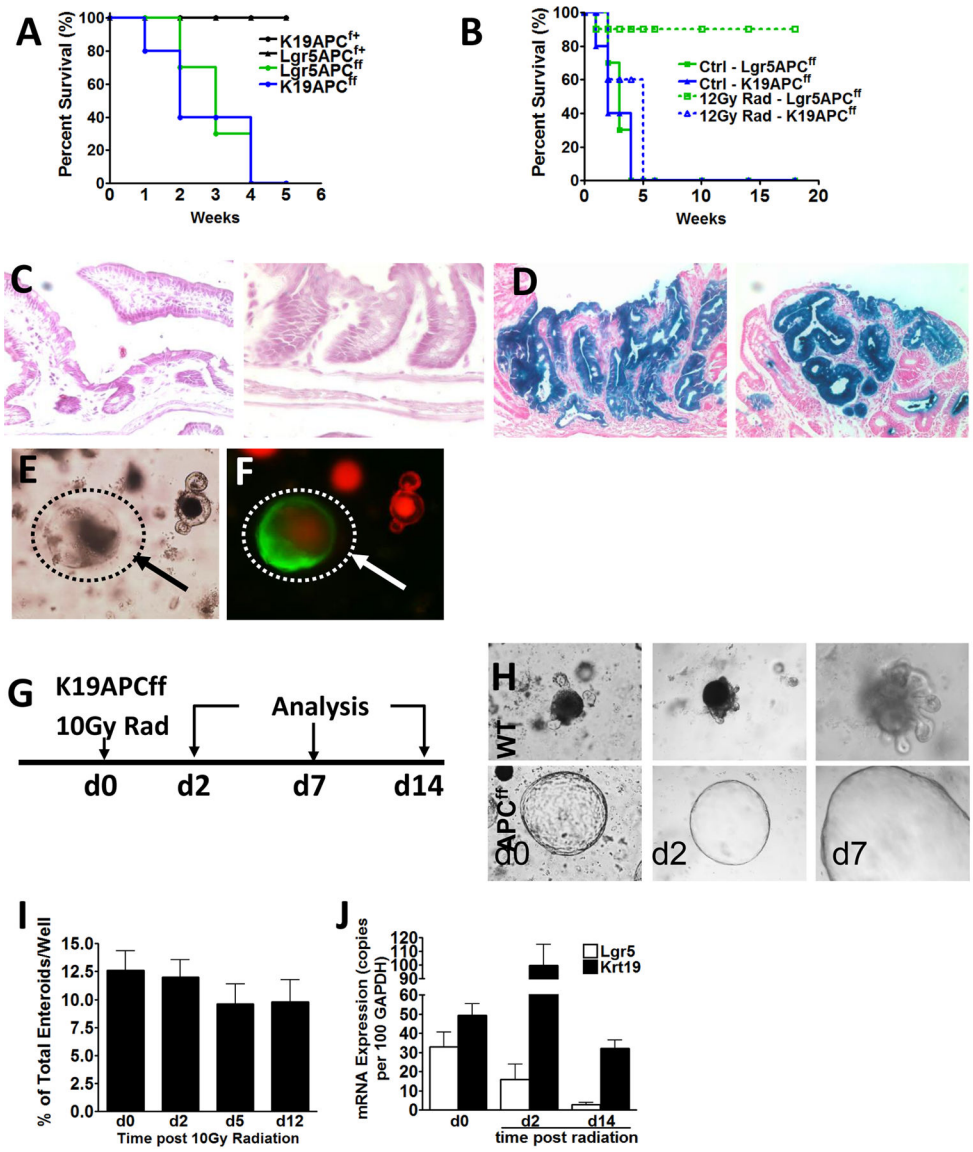

Figure 5. Radioresistant *Krt19*$^+$ cancer initiating cells are functionally distinct from *Lgr5*$^+$ stem cells

Krt19$^+$ and *Lgr5*$^+$ stem cells both serve as cancer initiating cells resulting in rapid mortality in *Krt19*-CreERT;R26-LacZ;ApcF/F or *Lgr5*-EGFP-IRES-CreERT2;R26-LacZ;ApcF/F mice (A). *Lgr5*-EGFP-IRES-CreERT2;R26-LacZ;ApcF/F mice irradiated 24h after tamoxifen show no mortality (B) and normal non-lineage traced intestine (left) and colon (right) (C). In contrast, *Krt19*-CreERT;R26-LacZ;ApcF/F mice irradiated 24h after tamoxifen continue to show rapid mortality (B) from intestinal (left) and colonic (right) tumors (D); (n ≥ 6 per group). Bright-field (E) and fluorescent (F) images of intestinal crypts from *Krt19*-CreERT;R26-mT/mG;ApcF/F cultured *in vitro* 24 h after tamoxifen. Note arrows point to recombined GFP$^+$ *Apc* floxed *Krt19*$^+$ cells appearing as spheroid structures. *In vitro* radiation protocol used to examine the effects of radiation injury on intestinal *Krt19*$^+$ cell derived *Apc* floxed tumor populations (G). *Krt19*$^+$ cell derived *Apc* floxed tumor populations pre (d0) and post (day 2 and day 7) radiation (10 Gy) (H). Quantification of

surviving *Krt19*$^{+}$ cell derived APC floxed enteroids pre and post radiation injury (I). *Krt19* and *Lgr5* mRNA expression levels in *Krt19*$^{+}$ cell derived *Apc* floxed enteroids pre and post radiation injury (J).

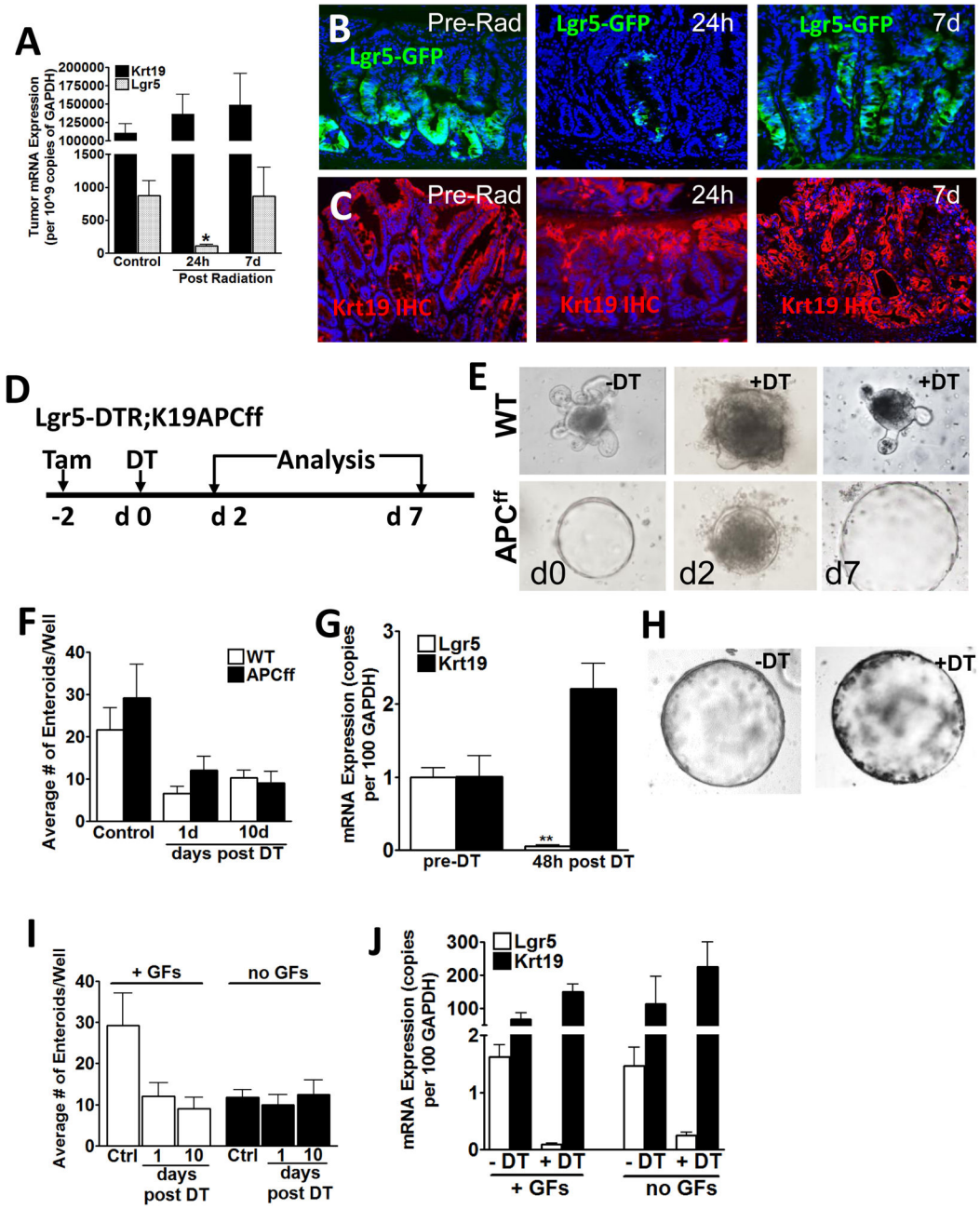

Figure 6. *Lgr5*$^{+}$ stem cells are radiosensitive within colonic tumors unlike *Krt19*$^{+}$ cells that are radioresistant

In vivo Krt19 and *Lgr5* mRNA in *Apc* floxed tumors pre or post (24h and 7 d) radiation (A); * indicates p<0.05 vs control; (n ≥ 4 per group). *Lgr5*-GFP^{+} (B) and *Krt19* immunopositive (C) cells in *Apc* floxed tumors pre or post radiation induced targeting of *Lgr5*$^{+}$ cells. *In vitro Lgr5*$^{+}$ cell ablation protocol used to examine the dispensability of *Lgr5*$^{+}$ cells in *Krt19*$^{+}$ cell derived *Apc* floxed enteroids from *Lgr5*-EGFP-DTR;*Krt19*-CreERT;Apc$^{F/F}$ mice (D). Bright-field images of intestinal enteroids from *Lgr5*-EGFP-DTR;*Krt19*-CreERT;Apc$^{F/F}$ mice pre (day 0) and post (day 2 and day 7) DT ablation of *Lgr5*$^{+}$ cells (E). Quantification of surviving *Krt19*$^{+}$ cell derived WT and APC floxed enteroids pre and post *Lgr5*$^{+}$ cell

ablation (F). *Krt19* and *Lgr5* mRNA expression levels in *Krt19*$^{+}$ cell derived APC floxed enteroids pre and post (48 h) *Lgr5*$^{+}$ cell ablation (G); ** indicates $p<0.01$ vs control; ($n \geq 4$ per group). Bright-field images of *Krt19*$^{+}$ cell derived APC floxed intestinal enteroids from *Lgr5*-EGFP-DTR;*Krt19*-CreERT;Apc$^{F/F}$ mice cultured in the presence (−DT) or absence (+DT) of *Lgr5*$^{+}$ cell ablation (H). Quantification of surviving *Krt19*$^{+}$ cell derived APC floxed enteroids pre and post *Lgr5*$^{+}$ cell ablation and cultured in the presence/absence of growth factors (I). *Krt19* and *Lgr5* mRNA expression levels in *Krt19*$^{+}$ cell derived APC floxed enteroids grown in the presence or absence of standard growth factors (R-spondin and noggin), pre and post (48 h) *Lgr5*$^{+}$ cell ablation (J); ($n \geq 4$ per group).